

Constant-pressure first-principles studies on the transition states of the graphite-diamond transformation

Y. Tateyama, T. Ogitsu, K. Kusakabe, and S. Tsuneyuki

Institute for Solid State Physics, University of Tokyo, Roppongi, Minato-ku, Tokyo 106, Japan

(Received 13 June 1996)

We have investigated the activation barriers and the intermediate paths of the transformation to cubic diamond and that to hexagonal diamond from graphite under pressure, allowing both atomic geometry and unit-cell shape to vary, in order to clarify the difference of the microscopic mechanisms between them. For this investigation, we have developed a method of finding a saddle point of the potential surface automatically on the basis of constant-pressure first-principles molecular dynamics. At the transition states, the length of the interlayer bonding is universal irrespective of the transformations and pressures, while there is a difference in the lateral displacement of atoms on the paths. It is found that the activation barrier from graphite to cubic diamond is lower than that to hexagonal diamond by ~ 70 meV/atom. These results suggest that, whenever collective slide of graphite planes is allowed, the transformation to cubic diamond is favored, and that hexagonal diamond can be obtained only when such slide is prohibited. [S0163-1829(96)06145-0]

5GPa = 5×10^9 Pa = 5万気圧 触媒をつかって2000 Kでグラファイトからダイヤモンドへ

I. INTRODUCTION

High-pressure synthesis of diamond from graphite (Gr) has been intensively studied because of its technological and fundamental importance. Many experiments for synthesis of cubic diamond (CD) have been carried out, so that methods and the P - T condition for the synthesis have been established empirically.¹ Industrially, the catalyst-solvent process under static conditions is usually utilized because this method allows us to make a large crystal in the manageable P - T region (~ 5 GPa and ~ 2000 K). Direct transformation to cubic diamond without catalysts, which is desired to make pure crystal, is also possible under shock-wave conditions or static compression at high temperature.

Furthermore, static compression at room temperature opens the possibility of different syntheses, namely, synthesis of hexagonal diamond (HD) which has a different stacking sequence of puckered hexagon from CD. (HD has AB stacking, while CD has ABC stacking.) Bundy and Kasper synthesized HD in the laboratory using well-crystallized graphite under static compression in the direction of the c axis up to 13 GPa.² Recently, Yagi *et al.* carried out an *in situ* x-ray diffraction study on the transformation of kish graphite at room temperature.³ They reported that the transformation took place at 14–18 GPa under quasihydrostatic pressure, and that the high-pressure phase was identified by the hexagonal diamond structure, where the c axis of HD was perpendicular to that of the initial graphite.

On the other hand, in recent experiments by Endo *et al.*,⁴ cubic diamond was observed by heating the sample up to ~ 800 °C under ~ 20 GPa after static compression of polycrystalline graphite at room temperature. Thus, under static compression at room temperature, there are two kinds of transformations from graphite, namely, those to cubic diamond and to hexagonal diamond. Although the difference of these two transformations might be attributed to the quality of the starting samples,⁴ the condition and the microscopic mechanism for each transformation are still unclear.

As to theoretical approaches for these transformations, there are some reports by means of first-principles calculations. Fahy *et al.* investigated the activation barriers at ambient pressure for the transformations from rhombohedral graphite (ABC stacking) to cubic diamond⁵ and from AA -stacking graphite to hexagonal diamond⁶ using a constant-volume scheme which fixes the shape of the unit cell. In those works, the transformation paths are assumed such that the orientation of the interlayer bonding is always parallel to the c axis of the initial graphite during the transformations. This assumption on the path is not the case in the experiment for the Gr-HD transformation.³ Recently, finite-temperature and pressure simulations of both Gr-CD and Gr-HD transformations with a constant-pressure scheme have been carried out by Scandolo *et al.*⁷ In that work, all the simulations were started from hexagonal graphite (AB stacking) without any assumptions on the path, and both transformations to CD and HD were observed. In addition, the orientation relation in the experiment³ was reproduced in the simulations for the Gr-HD transformation. However, since we cannot get good statistics from the limited number of dynamical simulations, characterization of the paths and estimation of the barriers are required to answer what condition is crucial for each transformation.

In this work, in order to clarify the difference of the transition probability and the microscopic mechanisms between the Gr-CD and the Gr-HD transformations, we have quantitatively investigated their transition states in the adiabatic potential surface under pressure. Actually, we calculate the activation barriers and the intermediate paths in both transformations at 0 and 20 GPa which correspond to the pressures below and above the critical one P_c for the transformations, respectively. From these results, we discuss the possibility and the mechanisms of the two transformations.

For the calculations, we have used the constant-pressure first-principles molecular dynamics (CP-FPMD) method which allows the shape of the unit cell as well as the atomic geometry to vary without any symmetry constraints. On the

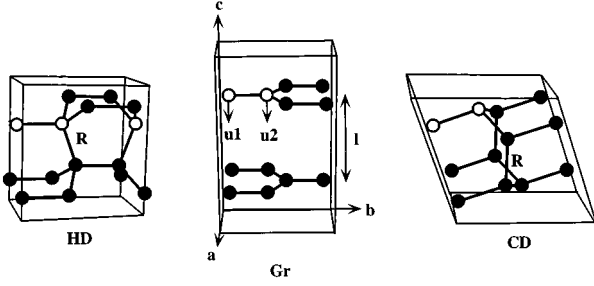


FIG. 2. Hexagonal diamond, graphite and cubic diamond in the monoclinic unit cell used in this work. The orientation in the conventional cell and the structural parameters $u1$, $u2$, R , and l are also displayed.

symmetry constraint during the simulations. The structures of the three phases in the unit cell are schematically displayed in Fig. 2. As to the structure of cubic diamond, deformation of the cell is necessary to express it within this unit cell of two layers because it has ABC stacking of puckered hexagon. From among some possible unit cells, we choose the one shown in Fig. 2, which has the smallest deformation.

The parameters to characterize the atomic geometry as well as cell parameters are also shown in Fig. 2. The parameters $u1$ and $u2$ indicate the displacement of the atoms perpendicular to planes. By the set of the parameters ($u1$, $u2$), one can distinguish the three phases. The set (0, 0) indicates graphite, while the sets (1/12, 1/12) and (1/16, -1/16) correspond to HD and CD, respectively. These two parameters are expressed with the internal coordinates in the unit cell. In addition, R is defined as the distance between atoms in adjacent layers which are connected by formation of sp^3 bonding, and l indicates the average of the interlayer distance defined as $csin\alpha$.

TABLE I. Optimized structural parameters at the (meta)stable state of each phase and at the activation barriers between them under external pressure $P_{\text{ext}}=0$ and 20 GPa in this work, compared with the experimental values indicated in brackets. The cell parameters a , c , and α in this table are in the monoclinic cell and definitions of other structural parameters are explained in the text.

	HD	HD-Gr barrier	Gr	Gr-CD barrier	CD
$P_{\text{ext}}=0$ (GPa)					
a (Å)	2.507 (2.51)	2.470	2.468 (2.46)	2.457	2.510 (2.51)
c (Å)	4.348 (4.36)	4.895	6.759 (6.70)	4.966	4.369 (4.36)
α (deg)	90 (90)	90	90 (90)	107.83	109.42 (109.42)
$u1$	0.0833 (1/12)	0.0482	0.0 (0)	0.0295	0.0624 (1/16)
$u2$	0.0833 (1/12)	0.0482	0.0 (0)	-0.0295	-0.0624 (-1/16)
R (Å)	1.542	2.073	3.453	2.085	1.545
l (Å)	2.174	2.447	3.380	2.364	2.060
$P_{\text{ext}}=20$ (GPa)					
a (Å)	2.466	2.444	2.427	2.442	2.472
c (Å)	4.290	4.795	5.614	4.904	4.301
α (deg)	90	90	90	106.52	109.21
$u1$	0.0834	0.0438	0.0	0.0277	0.0625
$u2$	0.0834	0.0438	0.0	-0.0277	-0.0625
R (Å)	1.522	2.077	2.895	2.091	1.523
l (Å)	2.145	2.398	2.822	2.351	2.031

B. Initial and final states

We first calculated the structures and the electronic properties of graphite, cubic diamond, and hexagonal diamond at 0 and 20 GPa which correspond to the pressures below and above the critical pressure for the transformations, respectively. The optimized structural parameters are compared with the experimental values at ambient condition in Table I. The results are in good agreement with experiments within error of 1%.

The total energies of HD and CD at 0 GPa are higher than that of Gr by 0.072 and 0.043 eV/atom, respectively. At 20 GPa, the relative enthalpies to graphite $\Delta H = H - H_{\text{Gr}}$ of HD and CD are found to be -0.208 and -0.234 eV/atom, respectively. Hence, our calculations lead to an energy relation consistent with the phase diagram of carbon at each pressure. These energy relations should not change even if zero-point motion energy is taken into consideration.¹⁶ Band gaps of Gr, HD, and CD are estimated ~ 0 , 3.12, and 4.11 eV, respectively. These results are consistent with the previous ones calculated with the LDA scheme.¹⁸

We also compare the total energy obtained here with those of the previous calculations.^{18,19} The difference of the total energy (0 GPa) between HD and CD is in good agreement with the previous results. On the other hand, the total energy of graphite might be underestimated due to the deficiency of k points in spite of sufficient cutoff energy. However, since our results show a consistent energy difference between HD and CD, we consider that this does not significantly affect the later discussion comparing the transformations to HD and CD.

C. Saddle-point search using the FI technique

Next we describe the search for the saddle points of the potential surface by means of the FI technique described in

Sec. II. As to the reference vector \mathbf{u} for the transformation to CD (HD), we adopted the direction to CD (HD) from orthorhombic graphite whose stacking manner is slightly different from hexagonal one within AB stacking. This is because the atomic geometry of orthorhombic graphite is closer to both CD and HD in the configuration space than that of hexagonal one so that this choice leads to less computational task. To check its validity, we compared energies of these two graphite structures. The difference of the total energy between them is less than 1 meV, which is beyond the accuracy of our calculations, and other electronic and structural properties are almost the same. In addition, this orthorhombic structure is the same as the intermediate one suggested by Scandolo *et al.*⁷ In fact, our simulations using the above reference vectors certainly converged.

In order to check whether the obtained states are on a saddle point or not, we then performed the usual structure optimizations starting from states shifted infinitesimally from the converged points. Since the structure changes into both sides of the transformation with a decrease of the enthalpy, we confirmed that the converged points are true saddle points. In these investigations, we carried out some simulations using the FI technique with changing the initial state in the intermediate possible region of the configuration space, and found that all the simulations give the same saddle point.

D. Transformation paths

The structural parameters at the obtained saddle points in both transformations under 0 GPa and 20 GPa are listed in Table I. At the saddle points, namely, the transition states, R has almost similar values, 2.07–2.09 Å, regardless of the transformations or external pressures. This suggests that a critical R seems to be universal in the transformations between sp^2 and sp^3 bonding of carbon. Thus, the transition states would be determined by the distance between atoms combining the adjacent layers.

As to the transformation paths to the saddle points, there is little difference in the reduction of the interlayer distance l and c -axis length. They are reduced from that of graphite similarly in both transformations such as 75% at 0 GPa and 60% at 20 GPa.

However, there exists a difference in the lateral displacement of atoms. Indeed, we can clearly see a difference in the deformation angle of the unit cell α . In the Gr-HD transformation, α retains 90° because of no change of stacking. On the other hand, α in the Gr-CD transformation already changes over 106.5° which is almost the same as that of CD. As to the out-of-layer displacement of atoms, u_1 and u_2 in the Gr-HD transformations change over 50% from Gr to HD, while those in the Gr-CD transformations rather have values closer to graphite. Thus, the collective sliding of the layers, which leads to the change of stacking, is necessary for reaching the saddle point in the Gr-CD transformation, while, because of no need to change of stacking, the local change of atomic configurations such as the buckling of planes is more required in the Gr-HD one.

E. Activation barriers

We next show the activation barriers in the transformations at the resulting saddle points. A schematic view of the

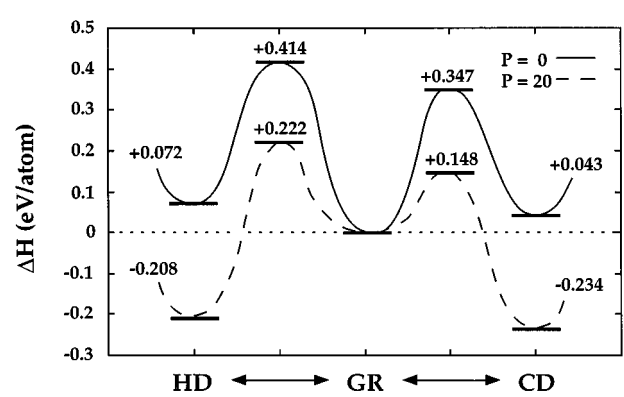


FIG. 3. Schematic view of the potential energy surface at 0 GPa with solid line and 20 GPa with dashed line. (The lines are a guide for the eye.) Relative adiabatic enthalpy $H = E + P_{\text{ext}}\Omega$ (eV/atom) to that of graphite is shown for each pressure.

hexagonal diamond graphite simple cubic

potential energy surface at 0 and 20 GPa is shown in Fig. 3, where the calculated values of the relative enthalpy to graphite, ΔH , are displayed. At 0 GPa, the activation barriers from graphite are 0.347 and 0.414 eV/atom for the transformations to CD and HD, respectively, while those at 20 GPa fall into 0.148 and 0.222 eV/atom. Thus, the activation barrier to CD is slightly lower than that to HD by 0.067 eV/atom at 0 GPa and 0.074 eV/atom at 20 GPa. In order to confirm the convergence of the barriers on the number of k points, we also carried out calculations with a larger k -point sampling (uniform 128 and 162 points) for the obtained barrier structures. As a result, the difference between the two barriers changed by less than 0.01 eV/atom in these calculations. This would ensure that the activation barrier for the Gr-CD transformation is lower than that for the Gr-HD one.

The barrier from Gr to CD at 0 GPa in this work is similar to the barrier between rhombohedral graphite and CD calculated by Fahy *et al.*,⁵ where the path is fixed so that the c axis is always parallel to that of the initial graphite during the transformation. This is because the transition state between Gr and CD obtained in this work without any constraints on the path has the structure with almost ABC stacking.

From the potential surface shown in Fig. 3, all the three phases can survive as metastable phases at ambient condition due to the existence of the high barriers between them at 0 GPa. Under high pressure, on the other hand, both barriers become sufficiently small for the state to go over at room temperature. By comparing these two transformations, it is confirmed that, at high pressure, the transformation to cubic diamond from graphite takes place under thermal equilibrium condition. Furthermore, from the viewpoint of chemical kinetics, the transition probability to cubic diamond is higher than that to hexagonal diamond even under nonequilibrium conditions because of the difference between the barrier heights. In fact, the transition probability to hexagonal diamond from graphite is approximately estimated as 10% of that to cubic diamond at room temperature under 20 GPa.

F. Discussion

Now we discuss the conditions and the microscopic mechanisms for both Gr-HD and Gr-CD transformations.